

# Ecological Partitioning and Morphometric Analysis of Two Sympatric Intertidal Gastropods (*Phorcus turbinatu* and *Patella caerulea*) in the Southern Mediterranean shore (Al-Hanyiah, Libya)

Munya Basheer Mohammed Eisay<sup>1</sup>, Ramadan A. S. Ali<sup>2</sup>, Sayed Mohamed Ali<sup>2,\*</sup>,  
Najiyah Salim Husayn Amdawi<sup>3</sup>

1: Departments of Marine Sciences, Omar AL-Mukhtar University, Albaida, Libya

2: Departments of Zoology, Omar AL-Mukhtar University, Albaida, Libya

3: Department of zoology, Universty of Derna, Alqubah, Libya

\*: Corresponding author [sayedmaiaaa@gmail.com](mailto:sayedmaiaaa@gmail.com)

doi: <https://doi.org/10.37745/ijfar.15/vol11n13149>

Published June 29, 2025

**Citation:** Eisay MBM, Ali RAS, Ali SM, and Amdawi NSH (2025) Ecological Partitioning and Morphometric Analysis of Two Sympatric Intertidal Gastropods (*Phorcus turbinatu* and *Patella caerulea*) in the Southern Mediterranean shore (Al-Hanyiah, Libya), International Journal of Fisheries and Aquaculture Research, 11 (1), 31-49

**Abstract:** This study investigated the distribution, abundance, and morphometric characteristics of two dominant intertidal marker species, the gastropods, *Phorcus turbinatu* and *Patella caerulea*, along the rocky shores of Al-Hanyiah in eastern Libya. Using 20 transects (1×1 m quadrats) spanning lower-mid littoral and shallow subtidal zones, we quantified population densities during autumn and measured key shell parameters (length, height, weight, base dimensions). *P. turbinatus* exhibited a conical shell (3–6 whorls; mean height = 19.19 mm, weight = 3.69 g) with distinctive black spiral markings and an operculum used to seal the shell aperture during low tide, conserving moisture and deterring predators, while *P. caerulea* displayed a whorl-less, striated shell (mean length = 19.93 mm, weight = 2.01 g). Both species showed negative allometric growth ( $b = 2.231$  and  $2.498$ , respectively), with strong correlations among morphometric traits. Spatial partitioning was evident: *P. turbinatus* dominated lower intertidal zones (peak abundance 0–3 m from shore), avoiding areas beyond 12 m landward or 3 m seaward. In contrast, *P. caerulea* distributed more broadly across mid-intertidal elevations (up to 14 m landward), with higher densities near the shoreline. Both species were completely absent from sandy substrates and exhibited no size gradients across their ranges. Behavioral differences reinforced niche separation—*P. turbinatus* utilized crevices and tidal pools for diurnal refuge, whereas *P. caerulea* relied on home scars and nocturnal activity. These patterns reflect adaptations to abiotic stressors (turbulence at high tide and overheating and desiccation at low tide) and resource competition, with *P. turbinatus* prioritizing mobility and *P. caerulea* optimizing attachment strength. Despite current minimal anthropogenic threats, future conservation efforts should monitor these keystone grazers, given their role in maintaining algal balance and microhabitat diversity. The study provides baseline data for assessing climate change impacts (e.g., ocean acidification, warming) on Mediterranean intertidal ecosystems.

**Keywords:** phorcus turbinatu, patella caerulea, niche partitioning, morphometric analysis, allometry, rocky shore ecology, mediterranean sea

## INTRODUCTION

The intertidal zone represents a critical ecotone between marine and terrestrial environments, characterized by extreme physical gradients including wave action, desiccation, salinity and temperature fluctuations (Branch, 1981). These areas exhibit stark contrasts between rocky and soft-bottom habitats: rocky shores support higher biodiversity with complex microhabitats (crevices, tide pools) that host diverse sessile and mobile organisms, while sandy intertidal zones are typically less diverse, dominated by burrowing species adapted to unstable substrates. Despite these challenges, both habitat types maintain unique assemblages of marine life, with their community structure shaped by the interplay of abiotic stressors and biotic interactions.

Gastropods serve as keystone species in these ecosystems. Grazers like *Phorcus turbinatu* and *Patella caerulea*, are ecologically marker species that regulate algal growth, maintain substrate heterogeneity, and provide microhabitats while serving as prey for intertidal carnivores (Coleman *et al.*, 2006). Their survival depends on distinct adaptations: *P. turbinatus*, a mobile trochid with a conical shell (3-6 whorls) and an operculum, exploits rocky crevices for refuge (Faidallah *et al.*, 2021), while the semi-sessile *P. caerulea* relies on home scars to resist desiccation and predation (Branch, 1981). These divergent strategies facilitate niche partitioning in sympatry.

Our study investigates the rocky-sandy intertidal system of Al-Hanyiah on Libya's eastern coast—a region that remains notably understudied despite its ecological importance (Boucetta, 2017; Hamad *et al.*, 2022)—as a representative model of the Southern Mediterranean shoreline. We aim to: (1) quantify distribution/abundance patterns of both species across the intertidal gradient; (2) analyze morphometric relationships (e.g., shell length vs. weight); and (3) identify coexistence mechanisms. We hypothesize distinct vertical zonation (*P. turbinatus* in lower zones, *P. caerulea* higher up) and negative allometric growth ( $b < 3$ ) reflecting energy allocation trade-offs.

These findings will illuminate how morphology mediates niche partitioning while providing baseline data for conservation in light of climate change (Fitzer *et al.*, 2019) and anthropogenic threats (Browne *et al.*, 2008) - particularly crucial for understudied Mediterranean ecosystems like Libya's.

## METHODS

The study site, Al-Hanyiah (32°51'N, 21°31'E; Fig. 1), is a traditional artisanal fishing landing area located on Libya's eastern coast (Reynolds *et al.*, 1995). Its intertidal zone consists of exposed, rugged rocky substrates—characterized by boulders, crevices, and small tidal pools—interspersed with sandy beaches, creating distinct ecological differences between the two habitats. This site is annually exposed to extreme temperatures and salinity gradients according to the different seasons of the year, creating dynamic environmental conditions that shape its biological communities.

The rocky shore exhibits high biodiversity, dominated by encrusting microalgae, gastropods (mainly limpets, top shells, and periwinkles), and tubeworm polychaetes. Faunal assemblages grow increasingly diverse from the mid-intertidal zone toward the lower shore. In contrast, the sandy shore supports lower biodiversity, primarily hosting bivalves.



**Fig. 1. The study site: Al-Hanyiah (Google map).**

### **Distribution and Abundance of *Phorcus turbinatu* and *Patella caerulea***

The distribution and abundance of live *Phorcus turbinatu* and *Patella caerulea* were assessed using a plastic rope belt transect (Figs. 2 and 3), deployed during daylight low tide perpendicular to the shoreline of Al-Hanyiah's rocky and sandy littoral zones. Each transect extended 3 m into the subtidal zone (nearshore sublittoral) and 20 m up the intertidal zone.

A total of 40 transects were established—20 on the rocky shore and 20 on the sandy shore—spaced 25 m apart, covering a 1 km longitudinal stretch of coastline (500 m per habitat). Sampling was conducted from September to November 2020 (autumn).

Within each transect, 12 consecutive 1×1 m quadrats were surveyed. All encountered *P. turbinatus* and *P. caerulea* were collected, stored in labeled plastic bags, and transported to the Marine Laboratory of the Zoology Department (Omar Al-Mukhtar University) for identification, counting, and measurement.

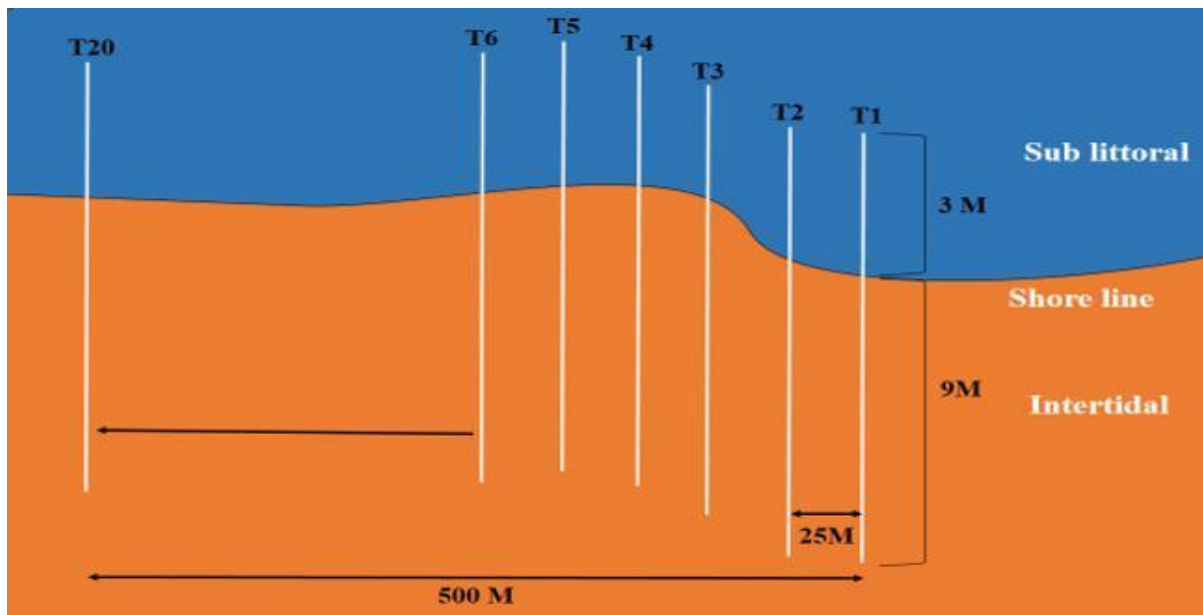


**Fig. 2.** The transect used in the study was made of 12 consecutive quadrats, each 1x1m. It was set 20 times (T1 – T20), 25-meter apart, 3m down the subtidal (sublittoral) and 20m up the intertidal, once in the rocky shore and once in the sandy shore.

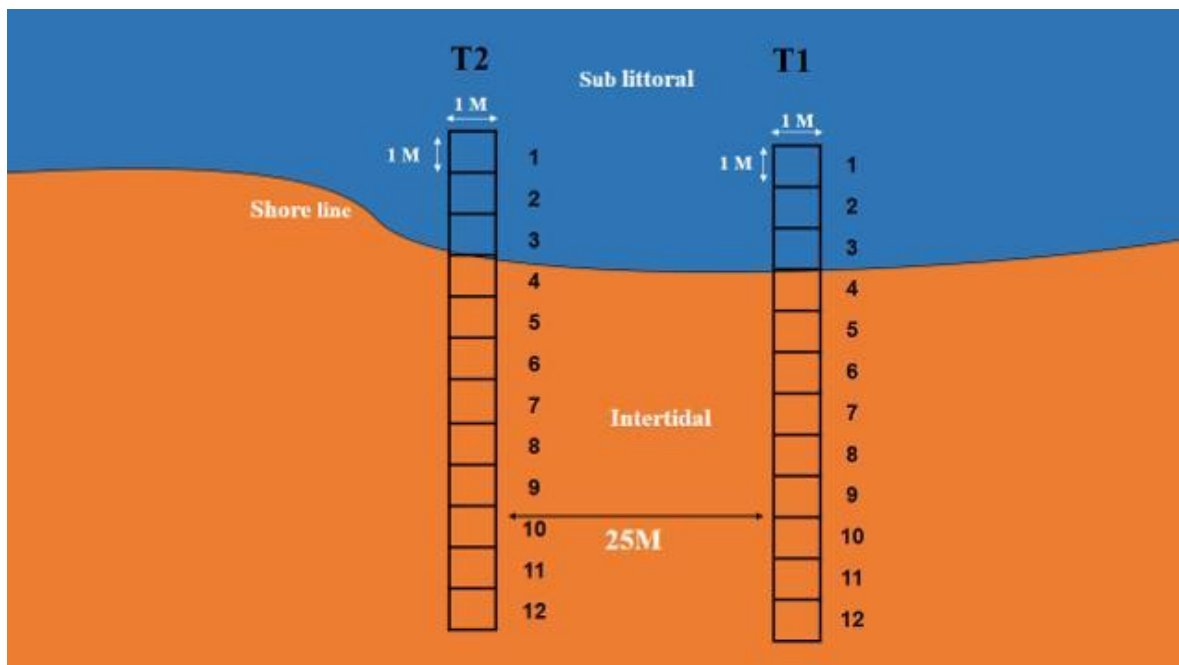


**Fig. 3.** Schematic representation of the sampling transect, comprising 12 contiguous 1×1 m quadrats aligned perpendicular to the shoreline. The transect spanned from 3 m depth in the subtidal zone (sublittoral) to 20 m elevation in the intertidal zone (only 12 are show in the diagram).

### Morphometric Analysis of *Phorcus turbinatu* and *Patella caerulea*

For each collected specimen, the following morphometric parameters were recorded (Fig. 4a & b):

- Total weight (W): Measured to the nearest 0.01 g using a precision digital balance.
- Shell dimensions: Height (H), length (L), base length (LO), and base width (W) to the nearest millimeter using a digital Vernier caliper.

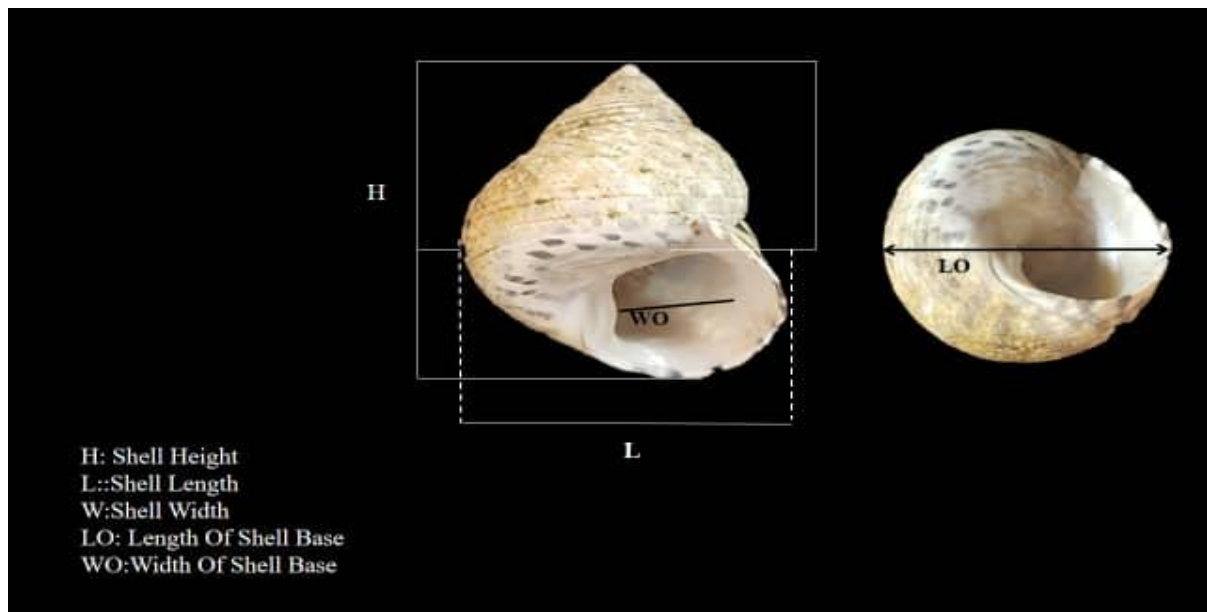


**Fig. 4a. Morphometric parameters measured for *Phorcus turbinatu*. L: Maximum shell length (apex to aperture); H: Maximum shell height (perpendicular to length); LO: Base length (longest dimension of attachment surface); WO: Base width (perpendicular to base length).**



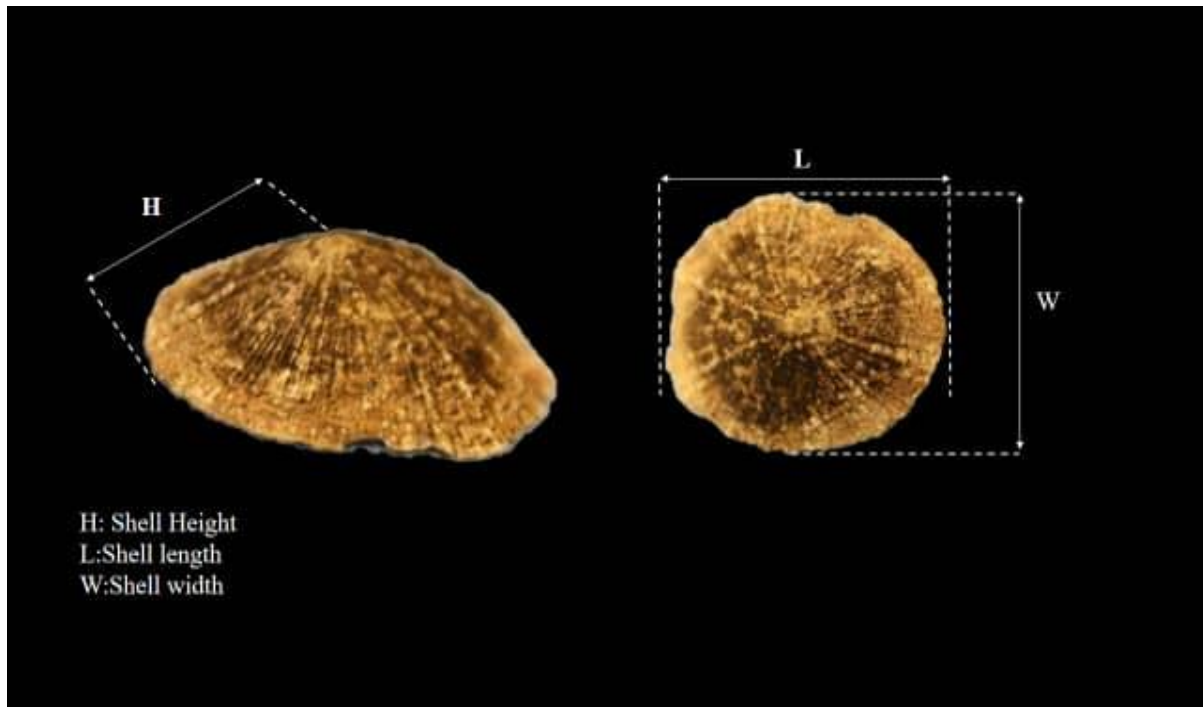


**Fig. 4b. Morphometric parameters measured for *Patella caerulea*. L: Maximum shell length (anterior-posterior axis); H: Maximum shell height (perpendicular to base plane); LO: Longest dimension of foot attachment surface; WO: Maximum width perpendicular to LO.**

#### **Binary correlations and growth relationships in *Phorcus turbinatu* and *Patella caerulea***

We analyzed pairwise Pearson correlations among morphometric parameters (total weight (W), shell height (H), shell length (L), base length (LO), and base width (WO)) for both *Phorcus turbinatu* and *Patella caerulea*.

To examine ontogenetic scaling relationships, we performed power, linear, and logarithmic regressions comparing (L) against the other parameters (W, H, LO and WO). These analyses used pooled data from all quadrats, with shell length serving as the growth indicator for both species.

### **Results**

#### ***Phorcus turbinatu***

##### **Results: Morphological Characteristics of *Phorcus turbinatu***

*Phorcus turbinatu* specimens collected from Al-Hanyiah were small trochids with rigid shells comprising 3-6 whorls, depending on size (Fig. 4a, Table 1). The shells exhibited a white base coloration, often overlaid with gray-green algal growth, and featured distinctive spirally arranged black rectangular markings. Shell height ranged from 5.40 to 47.77 mm (mean =

19.19 mm). Weight ranged from 0.06 to 18.40 g (mean = 3.69 g). Shell height (H): 16.93 mm; Shell length (L): 16.03 mm; Base length (LO): 16.03 mm; Base width (WO): 8.82 mm.

**Table 1. Descriptive statistics of *Phorcus turbinatus* total weight (W) in grams, and shell length (L), shell height (H), length of base (LO), and width of base (WO) in millimeters. St E: standard error; St D: standard deviation.**

	Minimum	Maximum	Mean	St E	St D
L (g)	5.40	47.77	19.19	.57	6.67
W (mm)	.06	18.40	3.69	.23	2.69
H (mm)	3.53	32.05	16.93	.50	5.85
LO (mm)	4.91	30.09	16.03	.42	5.01
WO (mm)	1.10	29.56	8.82	.44	5.20

#### **Binary correlations between morphometric parameters in *Phorcus turbinatu***

Pearson's correlation analysis revealed positive binary correlations between the measured morphometric variables of *Phorcus turbinatu*, with coefficients ranging from moderate to high (Table 2).

**Table 2. Pearson's correlation matrix for the measured parameters of *Phorcus turbinatu*: total weight (W), shell length (L), shell height (H), base length (LO), and base width (WO).**

	L	W	H	LO
W	0.586			
H	0.655	0.785		
LO	0.779	0.724	0.806	
WO	0.699	0.556	0.550	0.821

#### **Length-weight relationship in *Phorcus turbinatu***

The power regression of *Phorcus turbinatu* total weight (W) against shell length (L) yielded an allometric coefficient ( $b$ ) of 2.231, indicating negative allometric growth (Table 3; Fig. 5). A  $b$  value below the theoretical isometric threshold of 3 confirms that shell length increases at a faster rate than body weight during growth. In contrast, isometric growth ( $b = 3$ ) would imply proportional scaling of length and weight.

**Table 3. Regression models (power, linear, and logarithmic) of *Phorcus turbinatus* morphometric relationships: total weight (W, grams) and shell height (H), base length (LO), and base width (WO) (all in millimeters) regressed against shell length (L). *a* and *b*: regression constants; R<sup>2</sup>: coefficient of determination.**

<b>W vs L</b>	<b>a</b>	<b>b</b>	<b>R<sup>2</sup></b>
Power	0.004*	2.231**	0.588
Linear	-0.853	0.237*	0.344
Log	-8.475	4.214*	0.599
<b>H vs L</b>	<b>a</b>	<b>b</b>	<b>R<sup>2</sup></b>
Power	1.25*	0.881**	0.755
Linear	5.914	0.574*	0.655
Log	-15.131	11.103*	0.728
<b>LO vs L</b>	<b>a</b>	<b>b</b>	<b>R<sup>2</sup></b>
Power	1.485*	0.803**	0.824
Linear	4.86	0.584*	0.779
Log	-14.613	10.613*	0.814
<b>WO vs L</b>	<b>a</b>	<b>b</b>	<b>R<sup>2</sup></b>
Power	0.223*	1.212**	0.730
Linear	-1.632	0.545*	0.699
Log	-17.427	9.091*	0.671

\* Significant at 0.05 level.

\*\* Significant at 0.01 level.

Morphometric regressions against shell length in *P. turbinatus* Power, linear, and logarithmic regressions of shell height, base length, and base width against shell length (Table 3; Figs. 6–8) showed strong relationships, with coefficients of determination (R<sup>2</sup>) approaching 0.7. The power and logarithmic models provided better fits than the linear regression, as evidenced by their higher R<sup>2</sup> values.



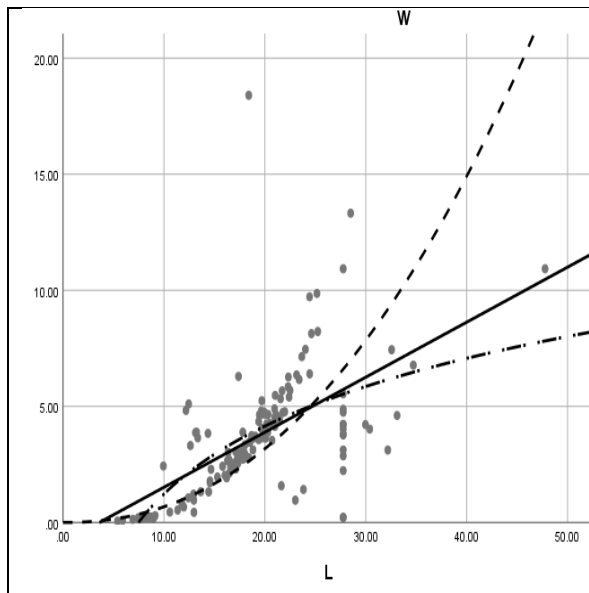


**Fig. 5. Regression models of total weight (W, gm) versus shell length (L, mm) in *Phorcus turbinatu*. (power: dashed line), (linear: solid line), (logarithmic: dotted dashed line)**

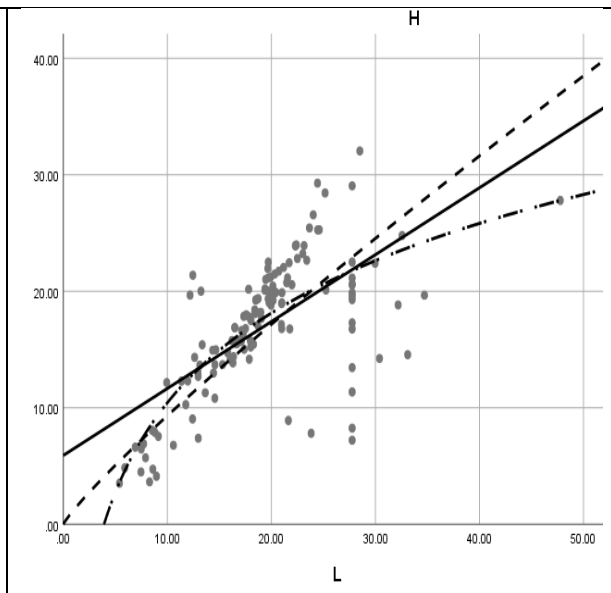


**Fig. 6. Regression models of shell height (H, mm) vs. shell length (L, mm) of *Phorcus turbinatu*. (power: dashed line), (linear: solid line), (logarithmic: dotted dashed line)**

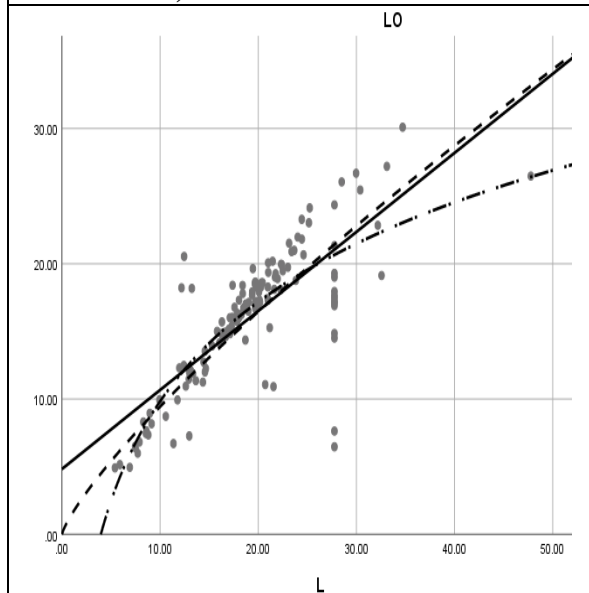


**Fig. 7. Regression models of base length (LO, mm) vs. shell length (L, mm) of *Phorcus turbinatu*. (power: dashed line), (linear: solid line), (logarithmic: dotted dashed line)**

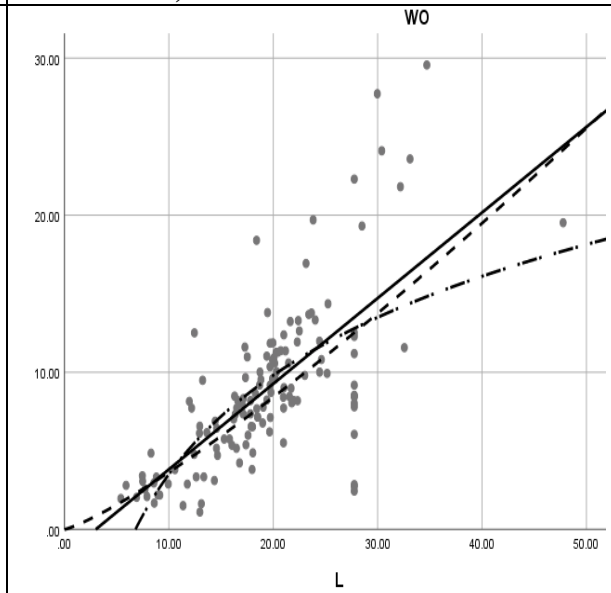


**Fig. 8. Regression models of base width (WO, mm) vs. shell length (L, mm) of *Phorcus turbinatu*. (power: dashed line), (linear: solid line), (logarithmic: dotted dashed line)**

### Distribution of *Phorcus turbinatu*

*Phorcus turbinatu* mainly inhabited the lower to mid intertidal regions of rocky shores of the study site. It was completely absent from sandy shores. Within the rocky shores, it was mostly abundant in the lower intertidal adjoining the shore (Fig. 9, quadrats 5 and 6). *P. turbinatus* became less abundant on moving away from the shore and upwards in the mid intertidal (quadrats 7 to 15). The snail was completely absent at 12 meters and more away from the shore. Within the sub tidal, *P. turbinatus* was only present at the first 3 meters of the submerged region (quadrats 2, 3 and 4), mostly in the region adjoining the shore (quadrat 4) and decrease in the direction of the sea (quadrats 3 and 2). *P. turbinatus* was completely absent at the submerged region that is more than 3 meters away from the shore (quadrat 1 and further in the infra-littoral).

Notably, no size-scaling patterns were observed across its distribution range (subtidal to mid-intertidal; Fig. 10).

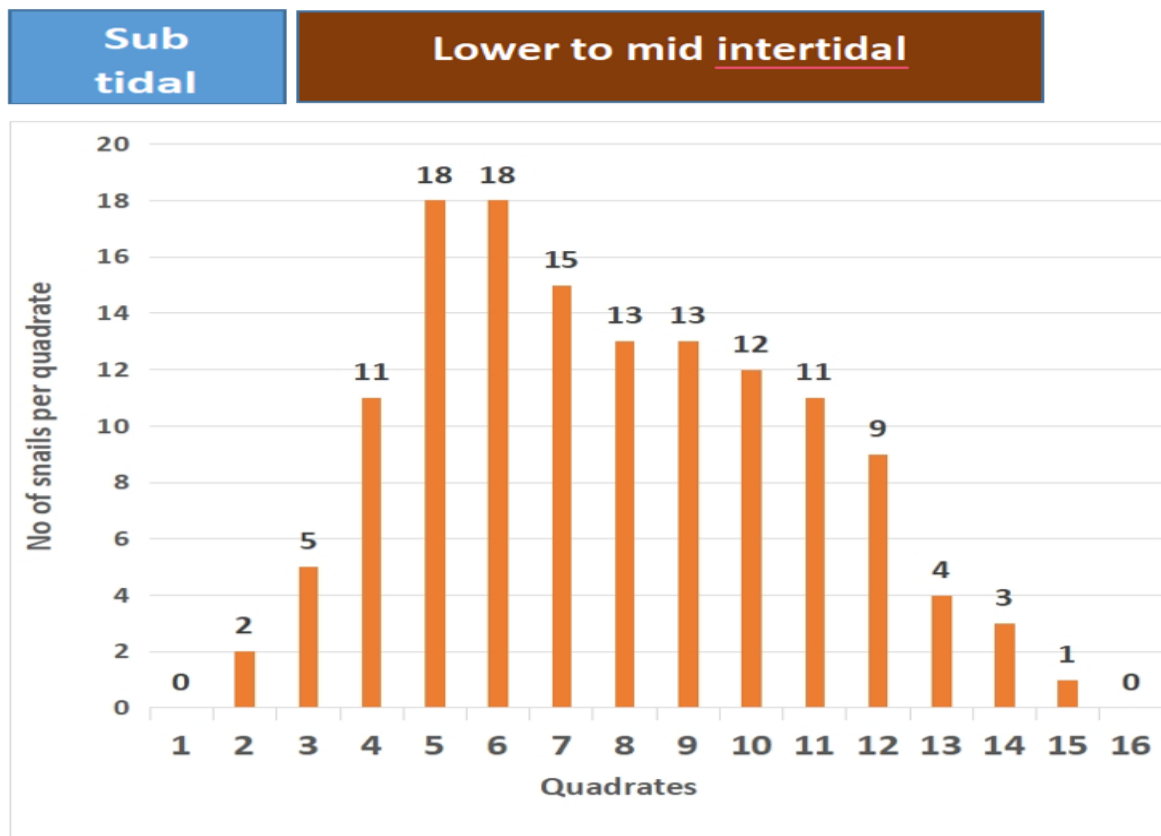


**Fig. 9.** Density distribution of *Phorcus turbinatu* (individuals (on top of columns) per quadrat (at base of columns)) across subtidal and intertidal zones.

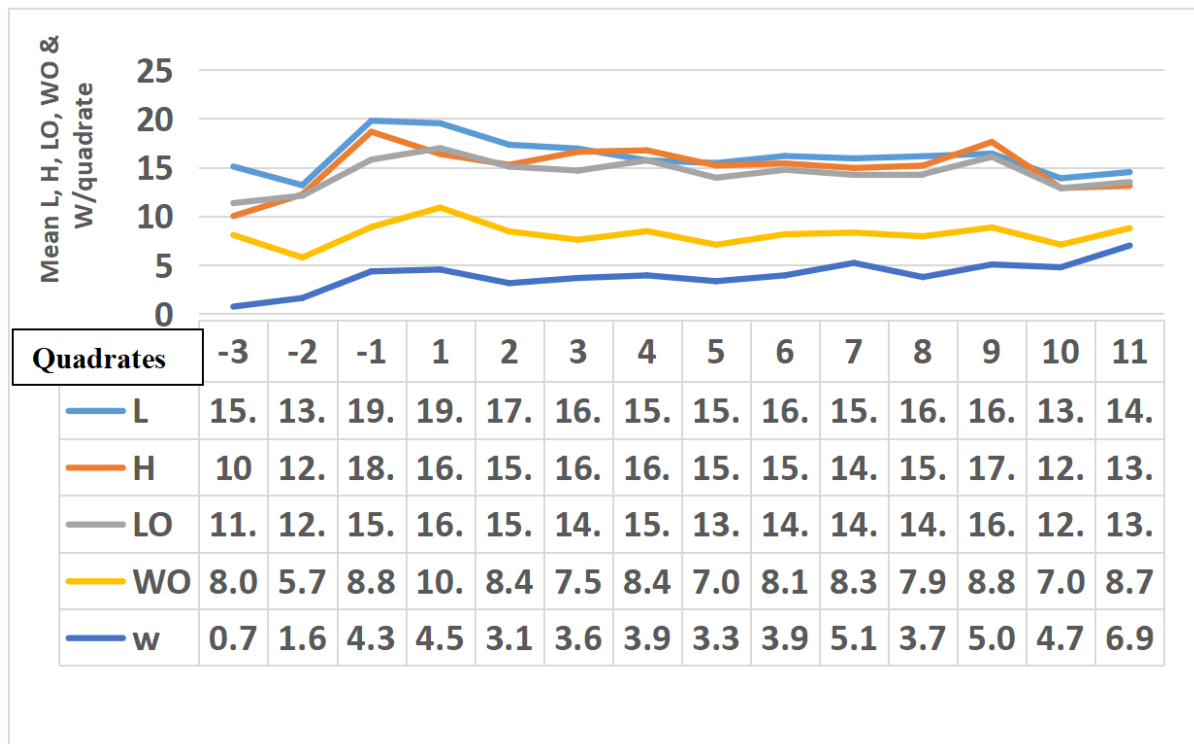


**Fig. 10.** Mean morphometric measurements (shell length (L), height (H), base length (LO), base width (WO) in mm; weight (W) in gm) of *P. turbinatus* per quadrat. Subtidal quadrats: -1 to -3. Intertidal quadrats: 1-11 (lower to mid-intertidal).

### *Patella caerulea*

#### Morphological Characteristics of *Patella caerulea*

The morphological traits of *Patella caerulea* in this study revealed small, top-shaped shells lacking whorls. While color varied, clean specimens were typically light brown with longitudinal striations. During low tides, *P. caerulea* firmly attached themselves to shallow depressions in rocks (scars) within the mid-to-lower intertidal zones of rocky shores.

The collected *Patella* specimens (Table 4) exhibited minimum, mean ( $\pm$  SE), and maximum lengths of 6.15 mm,  $19.928 \pm 1.181$  mm, and 31.77 mm, respectively. These lengths corresponded to weights of 0.06 gm,  $2.014 \pm 0.269$  gm, and 5.37 gm. The mean shell height, base length, and base width were 10.036 mm, 16.837 mm, and 14.033 mm, consecutively.

**Table 4. Descriptive statistics of *Patella caerulea* total weight (W) in grams, and shell length (L), shell height (H), length of base (LO), and width of base (WO) in millimeters. St E: standard error; St D: standard deviation.**

	Minimum	Maximum	Mean	St E	St D
<b>L (mm)</b>	6.15	31.77	19.928	1.181	7.186
<b>W (g)</b>	.06	5.37	2.014	.269	1.633
<b>H (mm)</b>	2.09	22.97	10.036	.9501	5.78
<b>LO (mm)</b>	5.31	29.05	16.837	1.034	6.289
<b>WO (mm)</b>	.50	29.45	14.033	1.328	8.078

#### **Binary correlations between the measured morphometric parameters**

All morphometric parameters showed strong positive correlations (Pearson's  $r = 0.667$ - $0.932$ ,  $p < 0.01$ ), Table 5.

**Table 5. Pearson's binary correlations between measured parameters of *Patella caerulea* (total weight (W), shell length (L), shell height (H), length of base (LO) and width of base (WO)).**

	L	W	H	LO
<b>W</b>	.814**			
<b>H</b>	.785**	.902**		
<b>LO</b>	.932**	.807**	.778**	
<b>WO</b>	.880**	.667**	.693**	.922**

\* significant at 0;05 level.

\*\* significant at 0;01 level.

#### **Length-weight relationship in *Patella caerulea***

The “b” value of the power regression of *Patella caerulea* total weight vs. shell length of 2.498 ( $R^2 = 8.24$ , a, and b significant at  $P = 0.05$  and  $0.01$ ) indicates negative allometric growth since it was less than 3, the theoretical value for isometric growth (Table 6 and Fig. 11).

**Table 6. Regression analyses (power, linear, and logarithmic) of morphometric relationships in *Patella caerulea*: total weight (W, g), and shell height (H), base length (LO), and base width (WO) in mm versus shell length (L, mm). "a" and "b" are constants of the regression line,  $R^2$ : coefficient of determination.**

<b>W vs L</b>	<b>a</b>	<b>b</b>	<b><math>R^2</math></b>
Power	0.001*	2.498**	0.824
Linear	-1.674*	0.185	0.663
Log	-6.521	2.928	0.578
<b>H vs L</b>	<b>a</b>	<b>b</b>	<b><math>R^2</math></b>
Power	0.252*	1.200**	0.605
Linear	-2.552*	0.632	0.632
Log	-19.259	10.051*	0.544
<b>LO vs L</b>	<b>a</b>	<b>b</b>	<b><math>R^2</math></b>
Power	0.947*	0.959**	0.861
Linear	0.578*	0.816	0.869
Log	-22.291	13.424*	0.820
<b>WO vs L</b>	<b>a</b>	<b>b</b>	<b><math>R^2</math></b>
Power	0.109*	1.583**	0.629
Linear	-5.674	0.989*	0.774
Log	-32.149	15.845*	0.692

\* significant at 0.05 level.

\*\* significant at 0.01 level.

### **Regressions of *Patella caerulea* measured parameters vs. shell length "L"**

Power, linear and logarithmic regressions of shell height, length of base and width of base vs. shell length of *Patella caerulea* (Table 6 and Figs. 12 to 14) were mostly strong ( $R^2$  close to 0.7 or above it). All "b" values were positive indicating that the concerned parameters increased during the growth of the top shell. The three regressions had equal reliability in describing the allometric relationships since they had comparable  $R^2$  values.



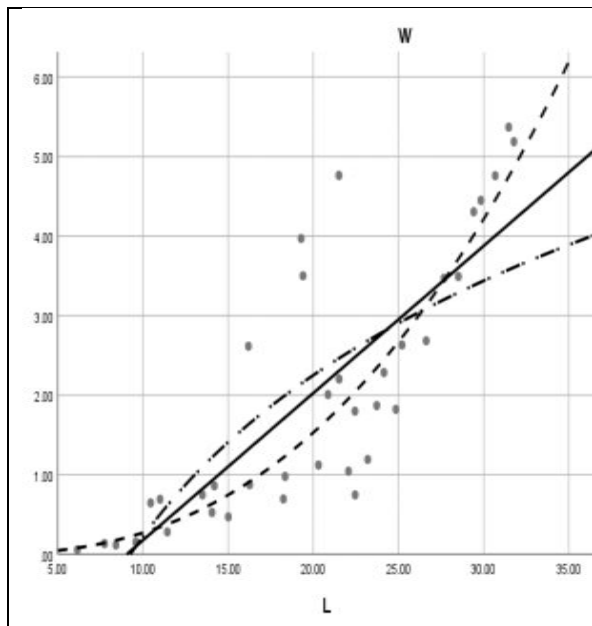


**Fig. 11. Regression models (power: dashed line), (linear: solid line), (logarithmic: dotted dashed line) of total weight (W, gm) versus shell length (L, mm) in *Patella caerulea*.**

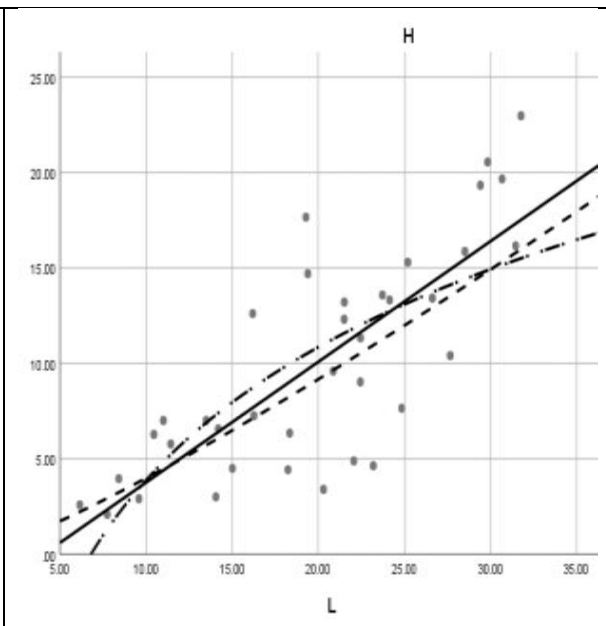


**Fig. 12. Regression models (power: dashed line), (linear: solid line), (logarithmic: dotted dashed line) of shell height (H, mm) vs. shell length (L, mm) in *Patella caerulea*.**

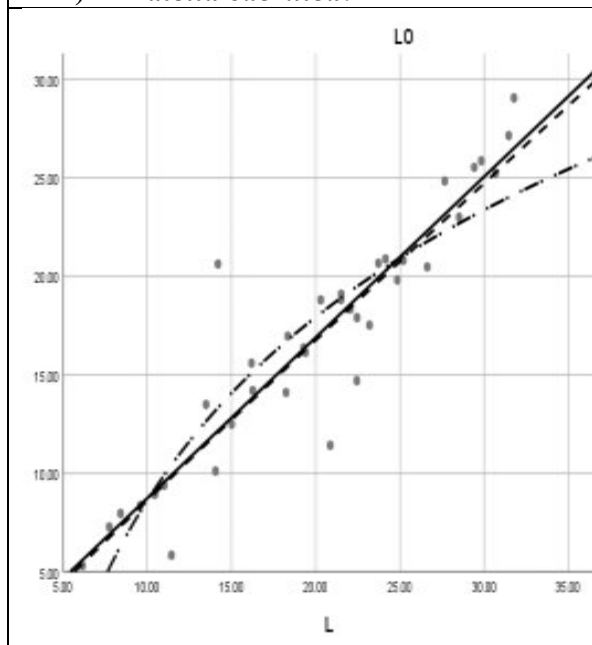


**Fig. 13. Regression models (power: dashed line), (linear: solid line), (logarithmic: dotted dashed line) of base length (LO, mm) vs. shell length (L, mm) in *Patella caerulea*.**

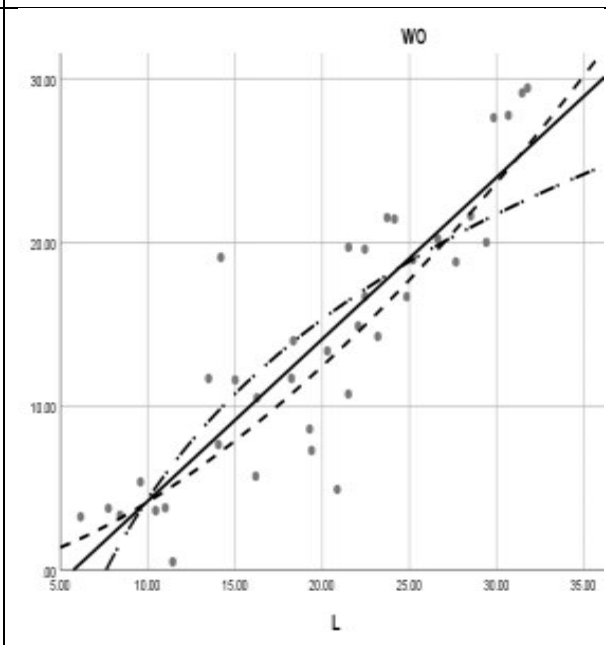


**Fig. 14. Regression models (power: dashed line), (linear: solid line), (logarithmic: dotted dashed line) of base width (WO, mm) vs. shell length (L, mm) in *Patella caerulea*.**

### Distribution of *Patella caerulea*

*Patella caerulea* inhabited the lower to mid-intertidal zones of rocky shores at the study site (Fig. 15). The species exhibited a broad distribution across the intertidal zone, extending up to 14 meters up shore. Unlike *P. turbinatus*, *P. caerulea* did not seek refuge in tidal pools during daytime low tides, as they relied on their "homes" (self-made scars) for dormancy; they were active exclusively at night. *P. caerulea* rarely ventured more than two meters from the shoreline into the sea and was absent from sandy shores.

On rocky shores, *P. caerulea* density decreased gradually with increasing distance from the shoreline toward the upper intertidal, disappearing entirely beyond 15 meters (Fig. 16, quadrats 14+). Within their distribution range—spanning the shallow subtidal to the mid-intertidal—*P. caerulea* showed no clear body size gradient (Fig. 16). However, larger individuals appeared to prefer the subtidal and lower intertidal zones closest to the shoreline (Fig. 15).

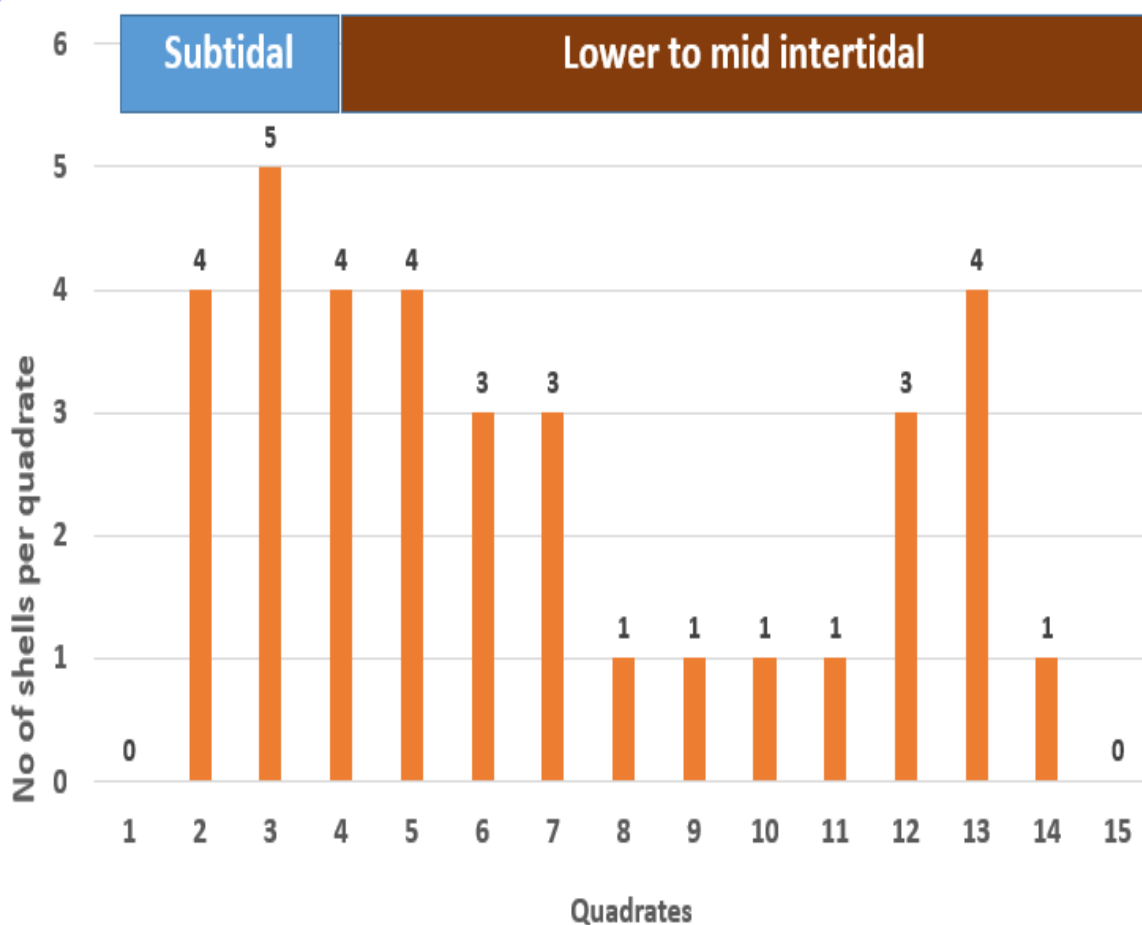


**Fig. 15.** Density of *Patella caerulea* (individuals (on top of columns) per quadrat (at base of columns)) in subtidal and lower to mid-intertidal zones.

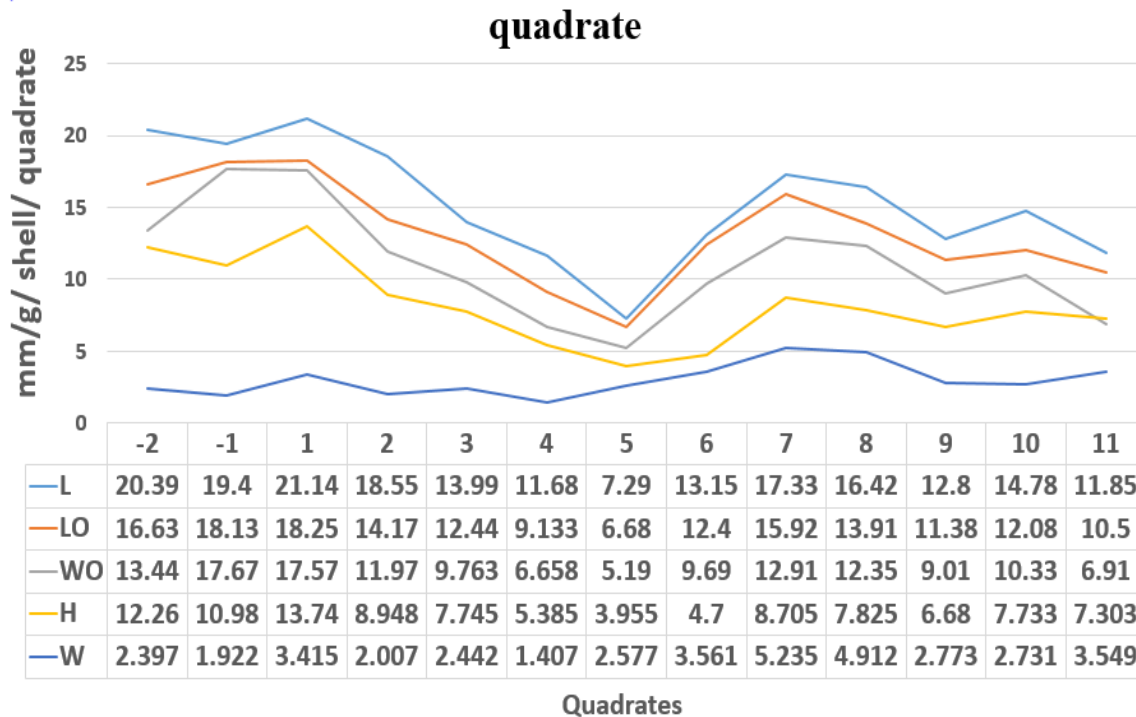


**Fig. 16. Mean shell dimensions (length [L], height [H], base length [LO], base width [WO] in mm) and weight (W in g) of *Patella caerulea* per quadrat. Quadrats -1 and -2 were located in the permanently submerged subtidal zone, while quadrats 1–11 spanned the lower and mid-intertidal zones.**

## DISCUSSION

The rocky intertidal zone of Al-Hanyiah, typical of the southern Mediterranean Seashore, supports two ecologically important marker gastropod species, *Phorcus turbinatu* and *Patella caerulea*, which exhibit distinct morphological and behavioral adaptations enabling their coexistence. *P. turbinatus*, a small mobile trochid (3–6 whorls), displays greenish-gray shells with microalgae and clay encrustation, averaging 16.93 mm in height and 3.69 g in weight—dimensions comparable to other Libyan populations (6.43–22.71 mm; 0.470–8.53 g; Faidallah *et al.*, 2021) but smaller than Algerian specimens (24.14–27.96 mm; 6.34–14.47 g; Boucetta, 2017). This size variation may reflect genetic differentiation arising from local environmental conditions, while the shell ornamentation likely serves both thermoregulatory and anti-predator functions (Faidallah *et al.*, 2021). In contrast, the semi-sessile *P. caerulea* (mobile but attached to home scars for most of its time) exhibits smaller dimensions (mean length 19.928 mm, weight 2.014 g) than reported elsewhere (Hamad *et al.*, 2022), with its homing behaviour and light-brown striated shell providing wave resistance, thermoregulation, and camouflage against rocky substrates (Hamad *et al.*, 2022) and thermoregulatory function.

These morphological differences underpin spatial segregation and resource partitioning. *P. turbinatus* dominates the lower midintertidal zone, where its conical shell facilitates mobility between tidal pools and crevices, offering protection from predators and desiccation during low tides (Faidallah *et al.*, 2021). However, this mobility comes at a cost: the species is vulnerable to wave action in exposed shallow subtidal areas, and its negative allometric growth ( $b = 2.231$ ) reflects a trade-off favoring shell elongation for agility over mass increase (Coleman *et al.*, 2006). Conversely, *P. caerulea* occupies higher elevations, with its flattened shell and broad foot enabling strong rock adhesion (Branch, 1981). Its less pronounced negative allometry ( $b = 2.498$ ) balances attachment strength with grazing efficiency (Espinosa *et al.*, 2009), a pattern consistent with global observations of intertidal gastropod communities (Boaventura *et al.*, 2002).

Behavioral strategies further reinforce niche partitioning. *P. turbinatus* exhibits diurnal activity, grazing on microalgae during low tide while retreating to crevices or tidal pools to avoid desiccation and predation (Williams *et al.*, 2011). During aerial exposure, it canseals its shell aperture with a horny operculum to conserve moisture—a critical adaptation complementing its use of microhabitat refuges.

Its mobility allows exploitation of ephemeral food resources, aligning with its negatively allometric growth strategy (Coleman *et al.*, 2006). In contrast, *P. caerulea* is primarily nocturnal, minimizing daytime exposure to predators and desiccation (Santini, *et al.*, 2005; Sempere-Valverde *et al.*, 2019; Martins *et al.*, 2010). Its semi-sessile nature—returning to home scars after foraging—enhances survival in high-energy intertidal zones (Branch, 1981). These temporal and behavioral differences reduce direct competition, allowing coexistence in overlapping but distinct microhabitats.

The complex topography of Al-Hanyiah's shoreline provides critical refuges exploited differentially by each species. *P. turbinatus* utilizes crevices and tidal pools to avoid overheating and desiccation at low tide and wave dislodgment at high tide (Williams *et al.*, 2011), while its algae-covered shells enhance crypsis (Faidallah *et al.*, 2021). *P. caerulea* relies on permanent home scars for attachment and moisture retention (Branch, 1981), with shell striations further camouflaging it against rocky substrates (Hamad *et al.*, 2022) and reflect heat rays during exposure. These adaptations reflect responses to environmental gradients: *P. turbinatus* tolerates wave shock but is susceptible to prolonged aerial exposure (Faidallah *et al.*, 2021), while *P. caerulea*'s morphology mitigates desiccation stress but increases vulnerability to overheating during extreme low tides (Williams *et al.*, 2011).

As keystone grazers present in abundance, both species significantly influence intertidal community structure. *P. turbinatus* regulates algal overgrowth, maintaining primary productivity and habitat complexity (Coleman *et al.*, 2006), while *P. caerulea*'s home scar creates microhabitats for sessile organisms (Martins *et al.*, 2010). However, their ecological roles face growing threats. *P. turbinatus* is vulnerable to shell dissolution from ocean acidification (Fitzer *et al.*, 2019), and *P. caerulea* risks thermal stress during increasing heatwave frequency (Williams *et al.*, 2011). Anthropogenic pressures, such as trampling and microplastic pollution (Browne *et al.*, 2008), compound these challenges, though local

exploitation levels remain unquantified. Comparative studies suggest further investigations are needed; for instance, the smaller size of *P. turbinatus* in Libya compared to Algerian populations (Boucetta, 2017) may reflect latitudinal gradients or local productivity limits, while *P. caerulea*'s reduced dimensions relative to Mediterranean conspecifics (Hamad *et al.*, 2022) could indicate genetic isolation or suboptimal grazing conditions.

Future research should prioritize quantifying grazing impacts on algal succession, monitoring emerging threats like microplastic ingestion, and assessing species-specific thermal and acidification tolerance limits. Conservation strategies must focus on preserving habitat heterogeneity and tidal pool availability while integrating studies on adaptive potential. By bridging local ecological knowledge with global change biology, we can better safeguard these keystone species and the intertidal communities they structure in a rapidly changing world.

## CONCLUSIONS AND RECOMMENDATIONS

### Conclusions

**Niche Partitioning:** *Phorcus turbinatus* and *Patella caerulea* exhibit distinct spatial distributions in Al-Hanyiah's intertidal zone, with *P. turbinatus* favoring lower zones and *P. caerulea* occupying mid-intertidal areas. This reflects adaptations to wave action, overheating, desiccation, and competition.

**Morphometric Differences:** Both species show negative allometric growth ( $b < 3$ ), with *P. turbinatus* prioritizing mobility (conical shell) and *P. caerulea* optimizing attachment (flattened shell). Strong correlations among shell dimensions highlight species-specific growth strategies.

**Behavioral Adaptations:** *P. turbinatus* uses crevices and opercula for diurnal refuge, while *P. caerulea* relies on home scars and nocturnal activity observed during the course of the present study. These behaviors reduce competition and enhance survival in harsh intertidal conditions.

**Conservation Concerns:** As keystone grazers, their decline could disrupt algal balance and microhabitat diversity. Climate change (acidification, warming) and human impacts (trampling, pollution) pose growing threats.

### Recommendations

**Extended Sampling:** Conduct day-night studies across seasons and tidal cycles to better understand behavioral and distributional dynamics.

**Climate Resilience Research:** Investigate species-specific tolerance to warming and acidification to predict future range shifts.

**Habitat Protection:** Prioritize rocky shore conservation, focusing on microhabitats (crevices, scars) critical for refuge and foraging.



**Comparative Studies:** Compare Libyan populations with Mediterranean counterparts to assess genetic or environmental drivers of observed size variations.

## REFERENCES

- Boucetta, S. (2017). Comparative study of morphometric traits in *Phorcus turbinatu* (Born, 1778) from different Mediterranean coasts of Algeria. *Mediterranean Marine Biodiversity*, 12(3), 201–210.
- Branch, G. M. (1981). The biology of limpets: Physical factors, energy flow, and ecological interactions. *Oceanography and Marine Biology Annual Review*, 19, 235–380.
- Browne, M. A., Dissanayake, A., Galloway, T. S., Lowe, D. M., & Thompson, R. C. (2008). Ingested microscopic plastic translocates to the circulatory system of the mussel, *Mytilus edulis*. *Environmental Science & Technology*, 42(13), 5026–5031.
- Coleman, R. A., et al. (2006). A continental scale evaluation of the role of limpet grazing on rocky shores. *Marine Ecology Progress Series*, 324, 235–246.
- Espinosa, F., Rivera-Ingraham, G. A., Fa, D., & García-Gómez, J. C. (2009). Effect of human pressure on population size structures of the intertidal limpet *Patella vulgata*: An approach for defining sustainable yield. *Marine Ecology Progress Series*, 382, 97–106.
- Faidallah, M. S., Al-Mahdawi, F., & Ramadan, K. (2021). Morphometric analysis and ecological distribution of *Phorcus turbinatu* (Born, 1778) along the Libyan coast. *Libyan Journal of Marine Science*, 5(1), 45–54.
- Fitzer, S. C., Phoenix, V. R., Cusack, M., & Kamenos, N. A. (2019). Ocean acidification impacts mussel control on biomineralisation. *Nature Climate Change*, 9(1), 40–44. <https://doi.org/10.1038/s41558-018-0346-z>
- Hamad, A., Al-Mahdawi, F., & Ramadan, K. (2022). Morphometric variation and ecological distribution of the limpet *Patella caerulea* along the Libyan coastline. *Journal of Mediterranean Marine Ecology*, 15(2), 112–125.
- Martins, G. M., Hawkins, S. J., Thompson, R. C., & Jenkins, S. R. (2010). Community structure and functioning in intertidal rock pools: Effects of pool size and shore height at different successional stages. *Marine Ecology Progress Series*, 329, 43–55.
- Reynolds, J. E., Haddoud, D. A., & Vall et, F. (1995). Prospects for aquaculture development in Libya, Lib-fish Field Document No. 9. Tripoli / Rome, FAO.
- Santini, G., Tendi, C., Righini, N., Thompson, R. C., & Chelazzi, G. (2005). Intra-specific variability in the temporal organisation of foraging of the limpet *Patella caerulea* on mesotidal shores. *Ethology Ecology & Evolution*, 17(1), 65–75. <https://doi.org/10.1080/08927014.2005.9522616>
- Sempere-Valverde, J., Sedano, F., Megina, C., García-Gómez, J. C., & Espinosa, F. (2019). Feeding behaviour of *Patella caerulea* L. and *P. rustica* L. under spring and neap simulated tides: An innovative approach for quick quantification of grazing activity. *Ethology Ecology & Evolution*, 31(2), 165–180. <https://doi.org/10.1080/03949370.2018.1561525>
- Williams, G. A., De Pirro, M., Leung, K. M. Y., & Morritt, D. (2011). Physiological responses to heat stress in the limpet *Cellana grata*: Can they explain its vertical zonation? *Journal of Thermal Biology*, 36(6), 371–375.